Journal of
Marine Science and Engineering

MDPI

Article

A Study on the Transport of ^{137}Cs and ^{90}Sr in Marine Biota in a Hypothetical Scenario of a Nuclear Accident in the Western Mediterranean Sea

Raúl Periáñez [1,*] and Carmen Cortés [2]

[1] Departamento de Física Aplicada I, Universidad de Sevilla, 41013 Sevilla, Spain
[2] Departamento de Matemática Aplicada I, Universidad de Sevilla, 41013 Sevilla, Spain; ccortes@us.es
* Correspondence: rperianez@us.es; Tel.: +34-954-486-474

Abstract: A Lagrangian model which simulates the transport of radionuclides released from nuclear accidents in the western Mediterranean Sea was recently described. This model was developed in spherical coordinates and includes three-dimensional mixing due to turbulence, advection by currents, radioactive decay, and radionuclide exchanges between water and bed sediments. Water circulation was downloaded from the HYCOM global ocean model. Water–sediment interactions were described using a dynamic model based on kinetic transfer coefficients. Mixing, decay, and water–sediment interactions were solved using a stochastic method. Now, a dynamic biological uptake model consisting of four species (phytoplankton, zooplankton, non-piscivorous fish, and piscivorous fish) has been integrated within the transport model to be able to assess the effects of a potential accident in biota and fishery regions. The model has been set up for ^{137}Cs and ^{90}Sr due to the radiological relevance of these radionuclides. Several hypothetical accidents were simulated, resulting in ^{137}Cs concentrations in biota significantly higher than background levels. In contrast, ^{90}Sr accumulates in the food chain to a considerably weaker extent.

Keywords: Mediterranean Sea; Lagrangian model; nuclear accident; biological uptake

Citation: Periáñez, R.; Cortés, C. A Study on the Transport of ^{137}Cs and ^{90}Sr in Marine Biota in a Hypothetical Scenario of a Nuclear Accident in the Western Mediterranean Sea. *J. Mar. Sci. Eng.* **2023**, *11*, 1707. https://doi.org/10.3390/jmse11091707

Academic Editor: Olivier Radakovitch

Received: 17 May 2023
Revised: 23 August 2023
Accepted: 28 August 2023
Published: 29 August 2023

1. Introduction

Models that simulate the transport of radionuclides in the marine environment have been developed since the pioneering works starting in the 1980s [1–4]. This topic has attracted more attention since the accident in Fukushima NPP (Nuclear Power Plant) in 2011, as can be seen in references [5–9], among many others.

More recently, several models that simulate the transport of radionuclides in the marine environment have been developed for areas that are potentially exposed to nuclear accidents, due to intense shipping activities or to the presence of nuclear facilities. These are the cases, for instance, of the Red Sea [10], the Arabian/Persian Gulf [11–13], the Indian Ocean [14], the eastern Mediterranean [15,16] as well as the western Mediterranean Sea [17]. All these works were motivated by projects launched by the International Atomic Energy Agency (IAEA), MODARIA, and MODARIA-II [18,19], which have highlighted the need to have numerical models ready to run in marine areas that could be potentially affected by a nuclear accident. The purpose is to be able to carry out a rapid assessment of an accident's aftermath.

Most of these models are Lagrangian in nature, because of their many advantages over Eulerian models when dealing with accidental releases into the sea as described in detail in the review in [20]. Essentially, Lagrangian models better handle the large concentration gradients that are involved in the case of accidental spills. Some earlier examples of Lagrangian models can be seen in [3,5,21,22]. Most models focus on transport processes in the water column and radionuclide interactions with sediments. Nevertheless, the uptake of radionuclides by marine biota is recently being considered and some models

already include a biological uptake model (BUM) integrated within the marine transport model [13,23–31].

A radionuclide transport model for the western Mediterranean Sea is described in [17]. The model is Lagrangian and developed in spherical coordinates. It includes three-dimensional mixing due to turbulence, advection by currents, radioactive decay, and interactions of radionuclides between water and bed sediments. It was applied, as examples, both to hypothetical accidents in a coastal NPP and to releases due to an accident in a nuclear vessel or a ship transporting nuclear waste.

The objective of the present work is to expand the radionuclide transport model for the western Mediterranean Sea described in [17] in such a way that contamination of marine biota can also be assessed. Thus, a BUM has been integrated into the marine transport model. It includes four species: phytoplankton, zooplankton, non-piscivorous and piscivorous fish; and parameters for ^{137}Cs and ^{90}Sr have been implemented. These radionuclides were selected due to their high bioavailability and hence radiological relevance: Sr chemistry is similar to Ca, thus accumulates in bones, and Cs is similar to K, thus accumulates in the flesh [29]. This is the fist time that this type of model is applied to the western Mediterranean.

The description of the model is summarized in Section 2 and some applications are presented in Section 3.

2. The Model

The Lagrangian transport model, developed in spherical coordinates, is described in detail in Periáñez and Cortés [17]. The model includes three-dimensional turbulent mixing, advection by three-dimensional currents, radioactive decay, and exchanges of radionuclides between water and seabed sediments. Decay, turbulent mixing, and water–sediment interactions are solved using a stochastic method. Water–sediment interactions are simulated through a dynamic kinetic model consisting of a single reversible reaction. Two kinetic coefficients, denoted as k_1 and k_2, describe the adsorption and release reactions, respectively. Additionally, the model calculates the ages of particles discharged to the sea and can also deal with both instantaneous and continuous releases of radioactivity. Full details can be found in [17] and are not repeated here.

The model domain covers the region from −5.80º to 9.00º in longitude and 34.50º to 44.50º in latitude (Figure 1). The water currents over this area were obtained from the HYCOM ocean model [32]. Several HYCOM application examples are presented on the model web page (https://www.hycom.org/) and specific applications to the Mediterranean Sea can be seen for instance in [33,34]. HYCOM has 32 vertical levels, and its horizontal resolution is 0.08º in longitude. Horizontal resolution is not uniform in latitude and ranges between 0.0659º and 0.0571º.

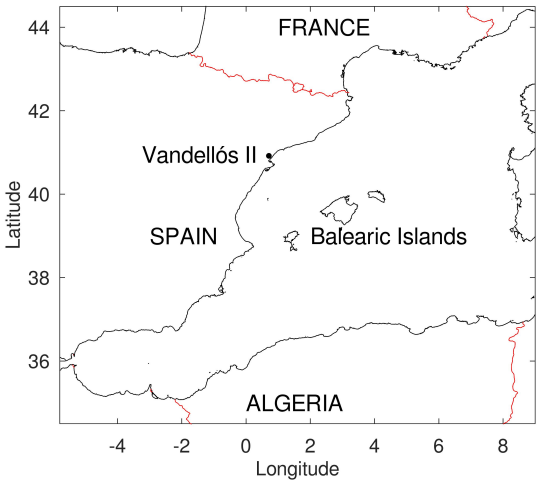

Figure 1. Model domain indicating Vandellós II NPP location, in Spain.

As described in detail in [17], the k_1 coefficient is deduced from the k_d distribution coefficient of each radionuclide and the value of the desorption coefficient k_2. Distribution coefficients, k_ds, are taken as the recommended values for coastal waters given by the IAEA [35]. The value of the desorption rate k_2 was obtained from Nyffeler et al. [36]: $k_2 = 1.16 \times 10^{-5}$ s^{-1}. It was used in many other previous modeling works carried out for different radionuclides (see for instance references included in the review in [20]).

The basic dynamic foodweb model used in this work consists of four types of marine organisms [25,28,29]: phytoplankton, zooplankton, non-piscivorous and piscivorous fish. The equation connecting the radionuclide concentration in predator C_{pred} (Bq/kg wet weight [WW]) with radionuclide concentration in food C_f (Bq/kg WW) is:

$$\frac{\partial C_{pred}}{\partial t} = aK_1C_f + bK_wC_w - K_{0.5}C_{pred}, \quad (1)$$

where K_1 (s^{-1}) is food uptake rate, a is the transfer coefficient through food, K_w is water uptake rate (s^{-1}), b is the transfer coefficient from water and finally C_w is activity concentration in water (Bq/m^3). The radionuclide elimination rate from the body of fish, $K_{0.5}$, is given by

$$K_{0.5} = \frac{\ln 2}{T_{0.5}}. \quad (2)$$

Here, $T_{0.5}$ is the biological half-life of the considered radionuclide. All species take radionuclides from water, phytoplankton is food for zooplankton, zooplankton is food for non-piscivorous fish and, finally, non-piscivorous fish is food for piscivorous fish. Phytoplankton takes radionuclides only with the water through adsorption and desorption processes. Since radioactivity presents a short retention time and rapid uptake, the radionuclide concentration in phytoplankton is obtained from an equilibrium approach [13,28,29]:

$$C_{phyto} = CR_{phyto}C_w, \quad (3)$$

where CR_{phyto} (m^3/kg, WW) is the concentration ratio for phytoplankton. It must be mentioned that fish movement in the sea is not considered in the present work. Only pelagic fish are considered in the model, defined as those living in a 50 m thick surface water layer, as in the models in [23]. A scheme representing the model can be seen in Figure 2.

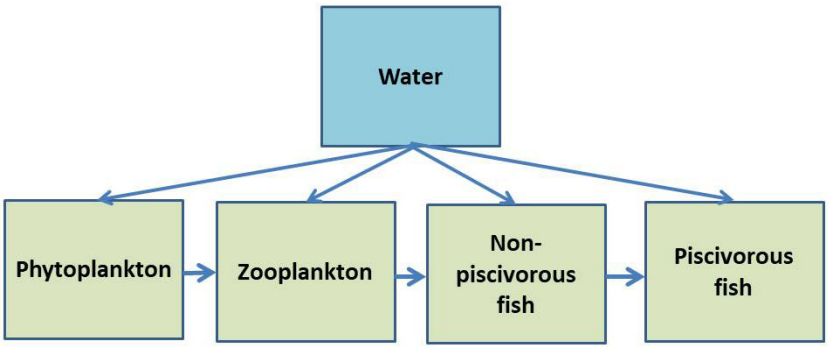

Figure 2. Scheme of the used BUM showing radionuclide transfers as arrows (adapted from [28]).

Please note that the Lagrangian transport model provides the radionuclide concentration in the water surface layer, C_w, in each grid cell from the number of particles within such cell at every time step during the model integration, as described in detail in [11,12,14] for instance. Then, the differential Equation (1) is solved (in a Eulerian framework) for each grid cell and each biota organism.

In the case of fish, the organ fraction f of the tissue that bioaccumulates each radionuclide must be considered. This target tissue depends on the radionuclide, being bones for ^{90}Sr and flesh for ^{137}Cs [29]. These organ fractions are given in Table 1 (see

for instance [28,30]). Thus, in the case of fish Equation (1) provides the radionuclide concentration in the target tissue, C_{tt}, and concentration in the fish is:

$$C_{fish} = fC_{tt} \quad (4)$$

Table 1. Organ fractions and biological half-lives for fish [13,28,30].

	^{90}Sr (Target Tissue: Bone)	^{137}Cs (Target Tissue: Flesh)
Organ fraction f	0.12	0.80
$T_{0.5}$ prey (days)	128	75
$T_{0.5}$ predator (days)	257	200

Standard literature values for all parameters in Equation (1) can be seen in Table 2. The concentration ratio for phytoplankton is $CR_{phyto} = 20 \times 10^{-3}$ m^3/kg in the case of ^{137}Cs and 1×10^{-3} m^3/kg for ^{90}Sr [35]. In the case of ^{90}Sr, $b = 1.0 \times 10^{-4}$ for zooplankton and $b = 3.0 \times 10^{-5}$ for fish [13,29]. Food and water uptakes depend on the metabolic rate of each species [27], thus some parameters are the same for ^{137}Cs and ^{90}Sr. As commented in the introduction, these radionuclides were considered due to their high radiological relevance, but BUM parameters for other radionuclides can be seen in [13,27].

Table 2. Parameters for the BUM [13,27–29].

	Zooplankton	Non-Pisc. Fish	Pisc. Fish
$T_{0.5}$ (day)	5	Table 1	Table 1
a (Cs–Sr)	0.2–0.2	0.5–0.29	0.7–0.29
b (Cs–Sr)	0.001–0.0001	0.001–3×10^{-5}	0.001–3×10^{-5}
K_1 (day^{-1})	1.0	0.035	0.0055
K_w (m^3/kg day)	1.5	0.1	0.075

Some information must be provided to the model for each specific simulation and each considered radionuclide: location of the accident (geographical coordinates), depth, date, duration, and magnitude of the release; simulation time; radionuclide k_d and decay constant and appropriate values for the BUM. All parameters are automatically defined after specifying the radionuclide of interest. The model can deal with either instantaneous or continuous releases. Output files are generated at the end of the simulated time. They consist of radionuclide concentration maps in the surface water layer, bed sediments, and radionuclide concentration maps in zooplankton, non-piscivorous and piscivorous fish. FAO (Food and Agricultural Organization of the United Nations) has divided the world ocean into several fishery areas. These fishery regions for the Mediterranean Sea are shown in Figure 3. The model provides the temporal evolution of radionuclide concentrations in surface water and biota in regions 1.1 and 1.2 (which are within the model domain) to assess the effects of potential accidents in these fisheries. It must be mentioned that averages over these relatively large regions cannot be used to assess the impact of an accident on fisheries during the acute phase of the releases, since very high concentrations are locally produced in the region close to the accident site and very small values far from it. However, averages can provide valuable information on the general trends of radionuclide concentrations at a longer temporal scale, when a high homogenization of the radionuclide patch is expected [14].

The number of particles used in the simulations is 2×10^6, but it can be changed. With this number of particles and for a one-year-long simulation, running time is about two hours in the case that the release is 90 days long.

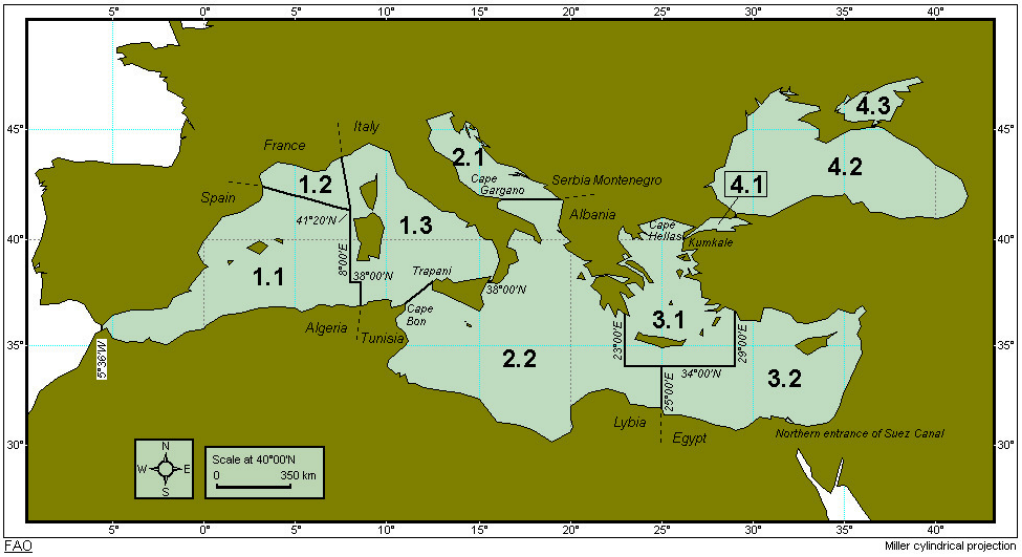

Figure 3. FAO major fishing areas of the Mediterranean Sea (from FAO web page).

3. Results

As mentioned in [17], it is not possible to make comparisons between model outputs and field measurements since hypothetical accidents were simulated. Nevertheless, the model formulation was tested in the frame of IAEA modeling intercomparisons exercises [19]. These exercises consisted of a comparison between models applied to simulate a hypothetical release (constant in time) from Fukushima NPP in the Pacific Ocean, to investigate the reasons for differences between models. Initially, a conservative radionuclide (not interacting with sediments) was considered, and, later, models were applied to ^{137}Cs including water–sediment interactions. Models were also compared using water circulation fields from different ocean models and the same circulation data; and using different and the same model parameters (diffusion coefficients, water–sediment interaction description, seabed topography, etc.). It was concluded that the main reason for discrepancies between model outputs was due to the description of water circulation. Full details of these exercises may be seen in [19].

However, the present formulation was also applied to real discharges in which measurements in water and sediment could be compared with model results, such as the real releases from Fukushima in the Pacific Ocean [23,37], releases from European nuclear fuel reprocessing plants (Sellafield, UK, and La Hague, France) into the Atlantic Ocean [38,39] and deposition due to the Chernobyl accident in the Baltic Sea [40].

Vandellós II NPP is located on the east Spanish coast, at coordinates 40º57′ N 0º52′ E (the location is indicated in Figure 1). The NPP consists of a 1087 MW power pressurized water reactor which started its operation in 1988. Some hypothetical releases of ^{137}Cs and ^{90}Sr from this NPP have been simulated.

Releases of ^{137}Cs have been studied first. All radionuclides are released in dissolved form. The releases were supposed to occur at the surface, with a magnitude equal to 1 PBq, lasting 90 days and being uniform in time. This is the same order of magnitude as the ^{137}Cs released from Fukushima NPP into the Pacific during the first three months after the nuclear accident in March 2011 [41]. Four hypothetical accidents have been analyzed, starting, respectively, on 21 March, 21 June, 21 September, and 21 December, to observe any seasonal effects in calculated transport pathways. It must be mentioned that atmospheric releases often occur in the cases of nuclear accidents (as described in [13] for instance). Radionuclides released into the atmosphere are later deposited on the surface of the sea, as in the Fukushima accident [41,42]. The model can also handle this atmospheric deposition, but only direct-release cases are presented.

Unlike what was carried out in [17], where 3-month simulations were carried out, in this paper the simulations have been extended to one year since the main goal is to observe the accumulation of radionuclides in biota.

Typical background levels of ^{137}Cs in water in the western Mediterranean, from measurements compiled in the IAEA MARIS database [43], are between 1 and 4 Bq/m^3. In the case of sediments, ^{137}Cs concentrations in the western Mediterranean range are 0.4–11 Bq/kg in the central sea and about 2 Bq/kg offshore northeast Spain. There are few data on ^{137}Cs in fish, but in the Northwestern Mediterranean concentrations are in the range of 0.1–0.2 Bq/kg (WW). In the Arabian Gulf, for instance, these background levels are lower, about 0.034 Bq/kg (WW) [44], a difference probably due to the influence of radioactive discharges through the Rhone River from the Marcoule nuclear complex in France. In the case of ^{90}Sr, concentration in water is about 1.7 Bq/m^3 [43], similar to that of, for instance, the Arabian Gulf [44].

Results for the ^{137}Cs release starting on 21 March are presented in Figure 4, which shows the calculated concentration in water, zooplankton, non-piscivorous and piscivorous fish. Due to the dynamic nature of the used BUM, radionuclide distribution in biota does not reflect that of water: there is a delay in the adsorption of radionuclides with respect to the concentration increase in water and biota remains contaminated during some time after a patch of contaminated water has traveled through a given area. It has been shown [45] that a dynamic model is more appropriate than an equilibrium model, based on concentration ratios, to describe radionuclide build-up in biota after a nuclear accident. In addition, concentrations resulting from this accident, both in water and fish, are significantly higher than background levels, reported above, along the northeastern Spanish coastline.

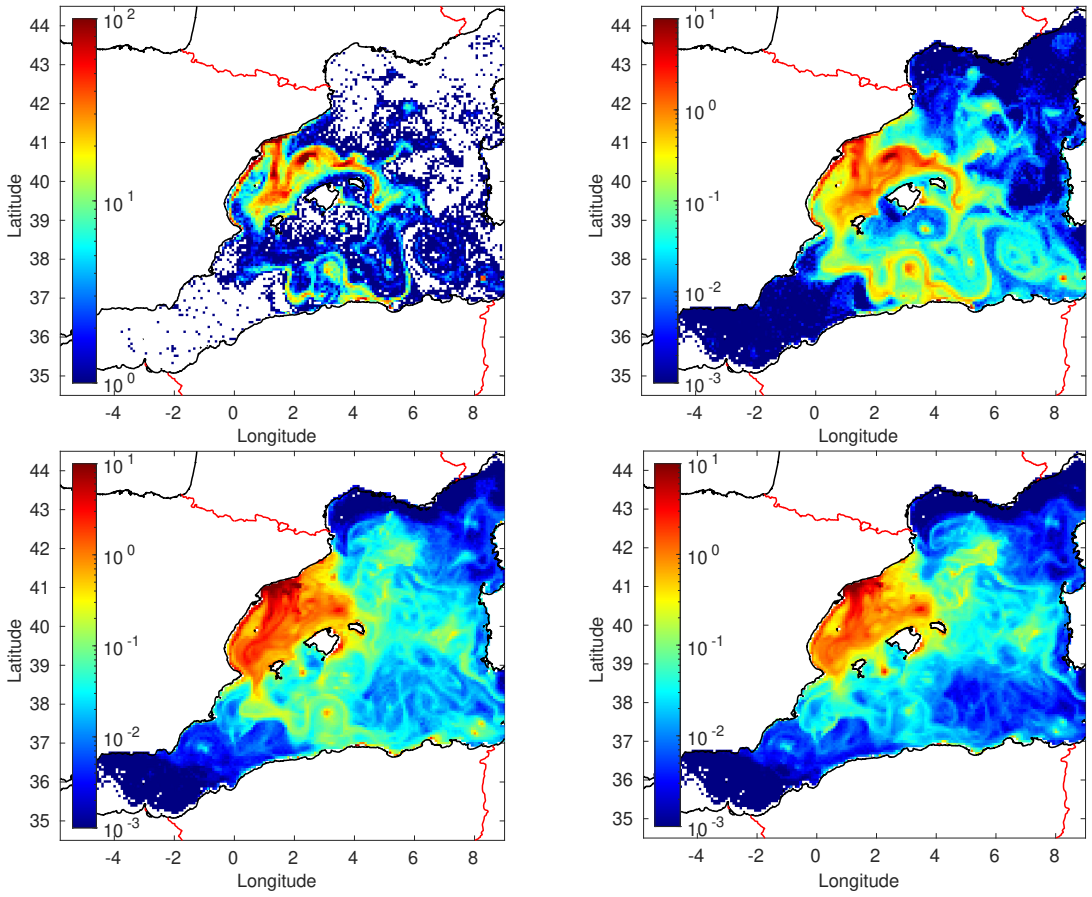

Figure 4. Calculated ^{137}Cs concentrations in surface water (Bq/m^3), zooplankton, non-piscivorous and piscivorous fish (Bq/kg WW)—from left to right and top to bottom—one year after a hypothetical accident in Vandellós II NPP starting on 21 March.

Time series of ^{137}Cs concentrations in water in FAO regions 1.1 and 1.2 can be seen in Figure 5 and do not show a clear temporal reduction after the accident since the western Mediterranean essentially is an enclosed sea. In Fukushima simulations [31] a rapid decrease in radionuclide concentrations in the coastal area was obtained, since releases took place in a dynamic coastal environment where radionuclides were quickly captured by the Kuroshio Current and efficiently exported to the open Pacific Ocean. Releases from Vandellós II occur in Region 1.1, thus concentrations in water are above zero from the initial time while it takes two months for radionuclides to reach Region 1.2. The delay in radionuclide build-up in biota with respect to water, due to the dynamic nature of the BUM commented above, can be seen in Figure 5.

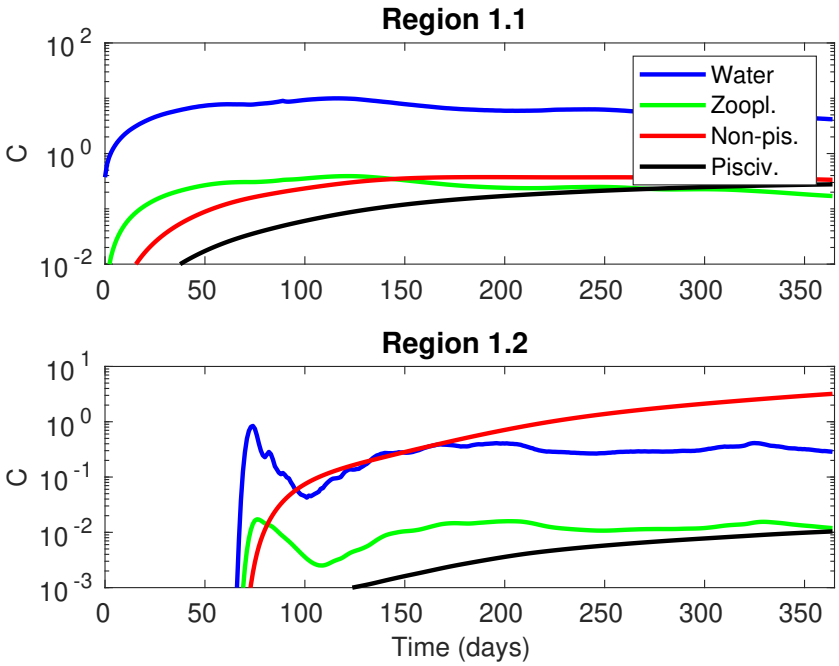

Figure 5. Calculated time evolution of ^{137}Cs mean concentrations in surface water (Bq/m^3), zooplankton, non-piscivorous and piscivorous fish (Bq/kg WW) in FAO regions for a hypothetical accident in Vandellós II NPP starting on 21 March.

Because releases from the NPP last 90 days and simulations are carried out over one year, final distributions of ^{137}Cs in water, sediments and biota do not show significant differences if the accident occurs in March, June, September, or December (seasonal differences were investigated at a shorter temporal scale in [17]). All results are presented in Supplementary Figures S1–S3, which show that as far as we move forward in the foodweb, seasonal differences become less pronounced. The time series of mean concentrations in FAO regions for the accident starting on 21 December are presented in Figure 6 as an additional example. In this case, nearly five months are required to achieve significant ^{137}Cs mean concentrations in Region 1.2.

In the case of sediments, radionuclides are distributed along the coastal sediments of the whole domain (Figure S4). Concentrations of the order of 10^5 Bq/kg, significantly larger than the background, are found along the northeast Spain coastline. In addition, results are essentially non-depending on the moment when the accident occurs since sediments act as radionuclide buffers and hence integrate the releases in time [46].

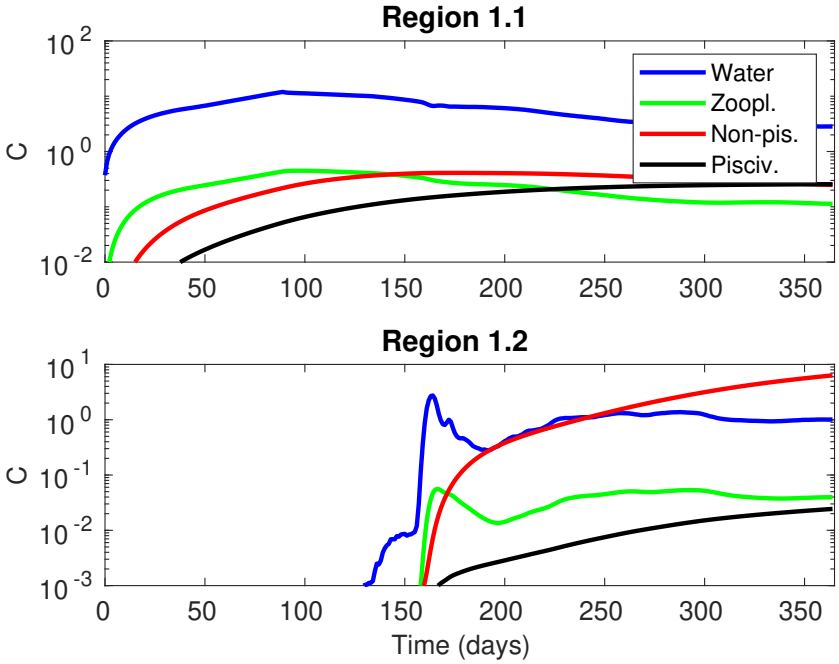

Figure 6. Calculated time evolution of ^{137}Cs mean concentrations in surface water (Bq/m^3), zooplankton, non-piscivorous and piscivorous fish (Bq/kg WW) in FAO regions for a hypothetical accident in Vandellós II NPP starting on 21 December.

The transport of ^{90}Sr was simulated for the same hypothetical accidents, although the total discharged amount was fixed as 100 TBq, which is the order of magnitude of the releases of this radionuclide from the Fukushima accident, as estimated in [47]. Calculated concentrations one year after the accident in water, zooplankton, non-piscivorous, and piscivorous fish are presented in Figure 7 for the accident starting on 21 June as an example. In the case of water, background level concentrations are obtained over most of the domain (about 1 Bq/m^3 as reported above), except along a segment of the Spanish coastline southwards from the NPP. Activity concentrations in biota are some orders of magnitude below those of ^{137}Cs, especially in the case of piscivorous fish. Indeed, Maderich et al. [13] have also noted in their model that ^{90}Sr does not significantly accumulate in the food chain. This can also be seen in Figure 8, where the temporal evolution of mean radionuclide concentrations in FAO regions are presented: mean concentrations in piscivorous fish are below the scale. It is also interesting to note that some oscillations in concentrations in water appear in Region 1.2. Since zooplankton takes radionuclides both from water and phytoplankton, which is at equilibrium with water, radionuclide concentrations in zooplankton follow the same oscillations as water. These oscillations are already lost in the case of fish, which shows a smooth increase in radionuclide concentrations.

It is interesting to note that, both for ^{137}Cs and ^{90}Sr, high concentrations (significantly higher than reported backgrounds) persist along the northeastern Spanish coastline even nine months after the releases have finished (Figures 4 and 7). This is due to the effects of sediments buffering radionuclides which are later released back to the water column [46]. Thus, sediments are acting as a long-term delayed source of radionuclides.

Calculated concentrations in bed sediments are significantly lower (up to three orders of magnitude) than those of ^{137}Cs, which is due to the low affinity of ^{90}Sr to be fixed to sediments (it has a smaller k_d than ^{137}Cs [35]). These results are presented in Figure S5, where it can be seen that only the Spanish coastline close to the NPP and the Balearic Islands are reached by radionuclides.

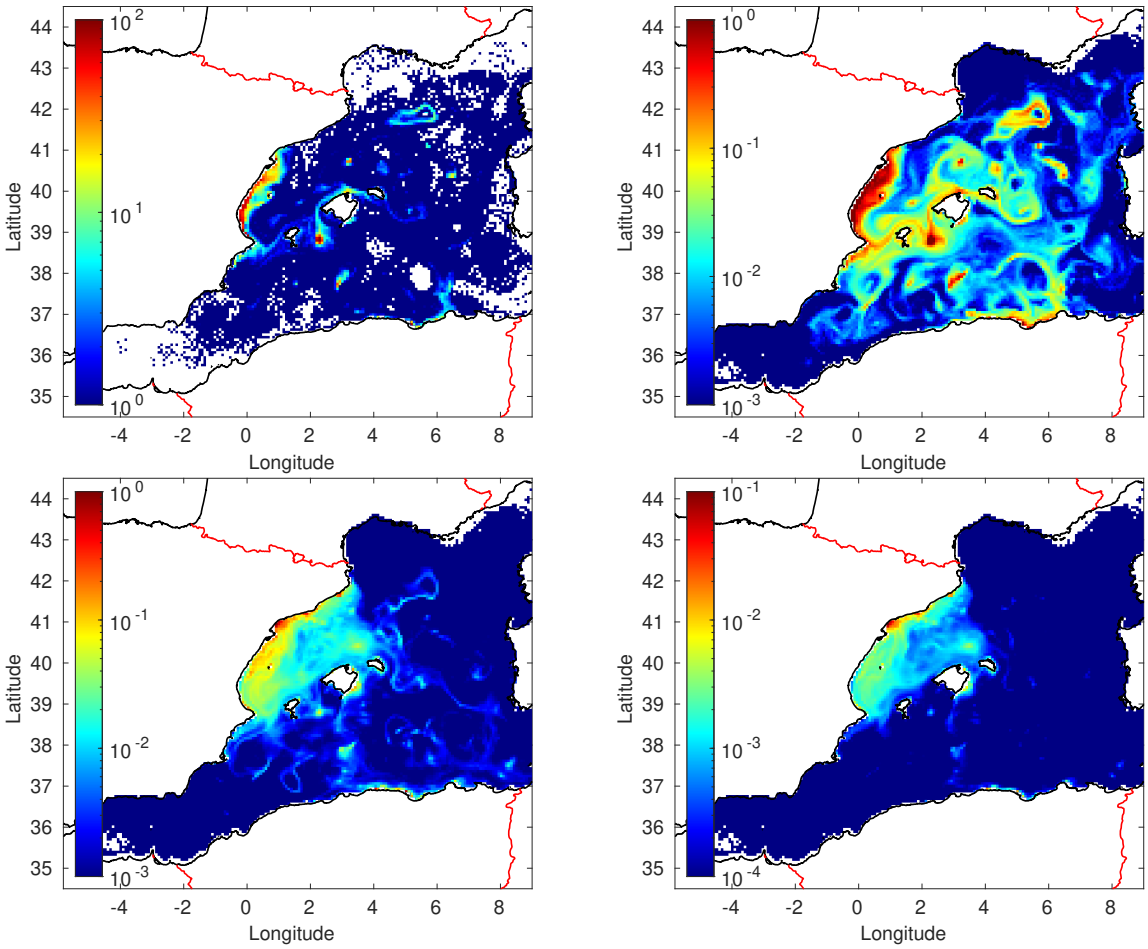

Figure 7. Calculated ^{90}Sr concentrations in surface water (Bq/m^3), zooplankton, non-piscivorous and piscivorous fish (Bq/kg WW)—from left to right and top to bottom—one year after a hypothetical accident in Vandellós II NPP starting on 21 June.

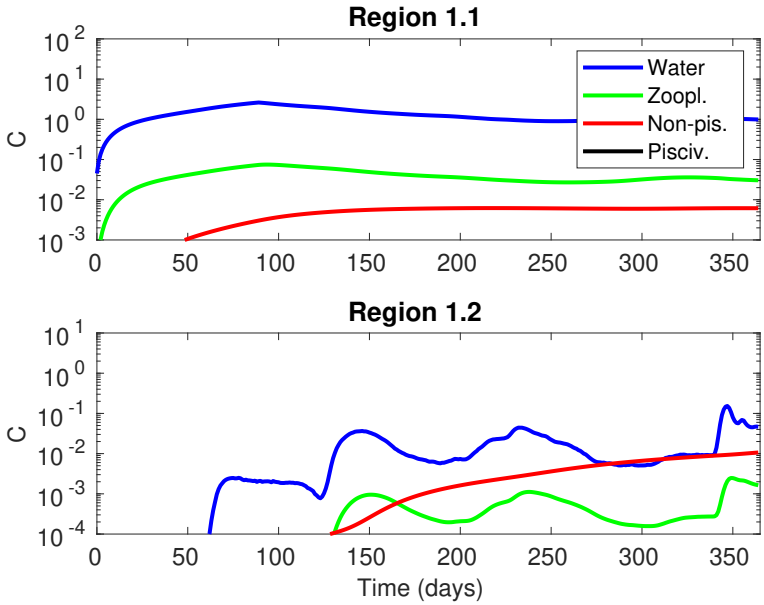

Figure 8. Calculated time evolution of ^{90}Sr mean concentrations in surface water (Bq/m^3), zooplankton, non-piscivorous and piscivorous fish (Bq/kg WW) in FAO regions for a hypothetical accident in Vandellós II NPP starting on 21 June.

Generally speaking, time series in Figures 5, 6 and 8 show variability in concentrations of Region 1.2 which is not apparent for Region 1.1. The reason is that Region 1.2 is much smaller than Region 1.1 (Figure 3) and is located north of the accident location. Thus, the calculated mean concentration is highly affected by circulation patterns, leading to abrupt increases as contaminated water comes into the region or decreases if water circulation makes such water leave Region 1.2. Time series variations in biota are softer than in water due to the dynamic nature of the BUM, as already commented.

A final example is described to show that the model also works for long simulations. For this purpose, the simulation of the accident described by Figures 4 and 5 was repeated but extending the simulated time to 20 years. The ^{137}Cs distribution in piscivorous fish after 20 years is presented in Figure 9. Maximum calculated concentrations occur at several spots mainly in the southwestern part of the Mediterranean and along the coastlines of Africa and Spain, close to the NPP. These persisting concentrations result in the same order of magnitude as reported background levels of the Persian Gulf, as mentioned above [13]. Minimum concentrations are found in the northern region.

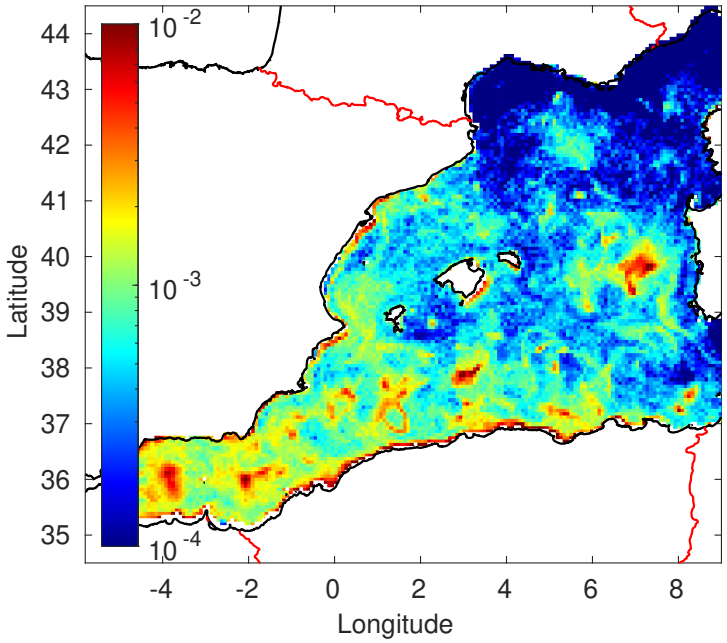

Figure 9. Calculated ^{137}Cs concentrations in piscivorous fish (Bq/kg WW) 20 years after a hypothetical accident in Vandellós II NPP starting on 21 March.

Finally, the time series of concentrations in FAO fisheries are presented in Figure 10. In the case of Region 1.1, there is a rapid reduction of mean concentration, and then a quite steady value is maintained. This also implies a very slow decrease in concentrations in biota, after the initial decreases which are delayed with respect to the decrease in water. The graphic for Region 1.2 shows an essentially constant concentration of water after the initial increase, which indicates an almost closed water circulation in this area. In this region, the mean concentration of fish reaches values above the aforementioned background levels.

The effective half-life, $T_{1/2}$, of a radionuclide in a marine region is defined as the time required for the mean radionuclide concentration in water to decrease in a factor 2 [14,48]. As depicted in Figure 10, concentration in water in Region 1.1 seems to exponentially decrease from day 120 onwards (in Region 1.2 it remains almost constant). This part of the curve was fitted to an exponential decay curve, resulting in a value $T_{1/2} = 0.47$ year with $r^2 = 0.9816$. This relatively long half-life, compared to that of the Indian Ocean [14], can be attributed to the fact that the western Mediterranean is a quite closed basin.

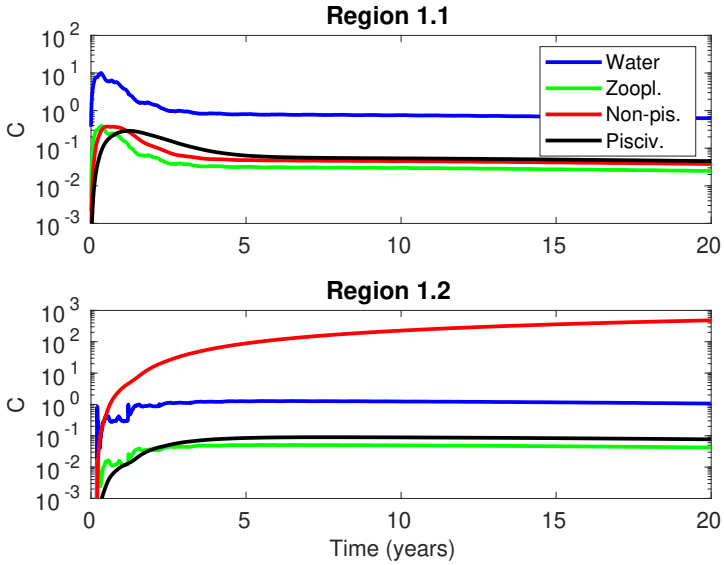

Figure 10. Calculated time evolution of ^{137}Cs mean concentrations in surface water (Bq/m^3), zooplankton, non-piscivorous and piscivorous fish (Bq/kg WW) in FAO regions for a hypothetical accident in Vandellós II NPP starting on 21 March in the case of a 20-year-long simulation.

4. Summary

A Lagrangian model that simulates the transport of radionuclides in the western Mediterranean Sea was presented in a previous publication [17]. Details of the physical model (advection by currents, three-dimensional mixing, radioactive decay, and exchanges of radionuclides between water and sediments) are described in such reference.

A dynamic biological uptake model, consisting of four types of marine organisms, has now been integrated within the marine transport model and setup for ^{137}Cs and ^{90}Sr. The model can be used to simulate either instantaneous or continuous radionuclide releases and it gives maps of radionuclide concentrations in water, sediments, and biota, as well as provides age distribution of radionuclides which can be useful to infer oceanographic information. Also mean radionuclide concentrations in FAO fisheries are calculated, both in water and in biota.

The model can be used as a rapid-response tool for decision-making after a radioactive spill in the western Mediterranean. Several radionuclides are released in a nuclear accident, but ^{137}Cs and ^{90}Sr were chosen to provide results of the biota uptake model due to their radiological relevance. As mentioned, only the radionuclide decay constant, k_d and release data must be modified in the model to make a particular simulation. In addition to the use of the model as a rapid-response tool for the initial phase after an accident, long-term simulations can be carried out as well. The output of this kind of model, providing radionuclide concentrations in different environmental compartments (water, sediment, phytoplankton, zooplankton, non-piscivorous fish, and piscivorous fish), can be complemented with specific tools for dose calculations, as for instance ERICA 2.0 software [49]. The model output can (1) support civil protection authorities to protect humans in the case of such a scenario, and (2) support research groups to better identify areas of interest for performing surveillance methods integrating in situ instrumentation onto fixed and/or mobile marine platforms.

Some application examples of the model are presented. Since simulations are carried out over one year, there are no significant differences in resulting concentration maps depending on the season when the hypothetical accident occurs. These differences are reduced as moving forward in the foodweb, i.e., the minimum differences are apparent for piscivorous fish. Calculated concentrations of both radionuclides in water are significantly higher than reported background values along the northeastern Spanish coastline, even one year after the accident. This must be attributed to the fact that sediments act as radionuclide buffers, these radionuclides are later released back to the water column. Thus, these

sediments behave as long-term delayed radionuclide sources. In agreement with previous work, it is found that ^{137}Cs is more effectively accumulated in the foodweb than ^{90}Sr. Thus, calculated ^{137}Cs concentrations in fish result higher than reported background values over a significant area of the western Mediterranean.

Supplementary Materials: The following supporting information can be downloaded at the following link: https://www.mdpi.com/article/10.3390/jmse11091707/s1, Figure S1: Calculated ^{137}Cs concentrations in surface water (Bq/m^3), zooplankton, non-piscivorous and piscivorous fish (Bq/kg WW) one year after a hypothetical accident in Vandellós II NPP starting on 21 June. Figure S2: Calculated ^{137}Cs concentrations in surface water (Bq/m^3), zooplankton, non-piscivorous and piscivorous fish (Bq/kg WW) one year after a hypothetical accident in Vandellós II NPP starting on 21 September. Figure S3: Calculated ^{137}Cs concentrations in surface water (Bq/m^3), zooplankton, non-piscivorous and piscivorous fish (Bq/kg WW) one year after a hypothetical accident in Vandellós II NPP starting on 21 December. Figure S4: Calculated ^{137}Cs concentrations in sediments (Bq/kg) one year after the four hypothetical simulated accidents. Figure S5: Calculated ^{90}Sr concentrations in sediments (Bq/kg) one year after the accident starting on 21 June.

Author Contributions: Conceptualization, R.P. and C.C.; Methodology, R.P.; Software, C.C.; Writing—original draft, R.P.; Writing—review & editing, C.C. All authors have read and agreed to the published version of the manuscript.

Funding: This research received no external funding.

Institutional Review Board Statement: Not applicable.

Informed Consent Statement: Not applicable

Data Availability Statement: Software available from authors.

Conflicts of Interest: The authors declare no conflict of interest.

Abbreviations

The following abbreviations are used in this manuscript:

BUM	Biological Uptake Model
FAO	Food and Agriculture Organization of the United Nations
NPP	Nuclear Power Plant
WW	Wet Weight

References

1. Prandle, D. A modelling study of the mixing of 137 Cs in the seas of the European Continental Shelf. *Philos. Trans. R. Soc. Lond. Ser.* **1984**, *A310*, 407–436.
2. Breton, M.; Salomon, J.C. A 2d long-term advection–dispersion model for the Channel and southern North-Sea. A: Validation through comparison with artificial radionuclides. *J. Mar. Syst.* **1995**, *6*, 495–513. [CrossRef]
3. Harms, I.; Karcher, M.J.; Dethleff, D. Modelling Siberian river runoff – implications for contaminant transport in the Arctic Ocean. *J. Mar. Syst.* **2000**, *27*, 95–115. [CrossRef]
4. Sánchez–Cabeza, J.A.; Ortega, M.; Merino, J.; Masqué, P. Long-term box modelling of ^{137}Cs in the Mediterranean Sea. *J. Mar. Syst.* **2002**, *33*, 457–472. [CrossRef]
5. Kawamura, H.; Kobayashi, T.; Furuno, A.; In, T.; Ishikawa, Y.; Nakayama, T.; Shima, S.; Awaji, T. Preliminary numerical experiments on oceanic dispersion of ^{131}I and ^{137}Cs discharged into the ocean because of the Fukushima Daiichi nuclear power plant disaster. *J. Nucl. Sci. Technol.* **2011**, *48*, 1349–1356. [CrossRef]
6. Behrens, E.; Schwarzkopf, F.U.; Lubbecke, J.; Boning, C.W. Model simulations on the long-term dispersal of ^{137}Cs released into the Pacific Ocean off Fukushima. *Environ. Res. Lett.* **2012**, *7*, 034000. [CrossRef]
7. Tsumune, D.; Tsubono, T.; Aoyama, M.; Hirose, K. Distribution of oceanic ^{137}Cs from the Fukushima Daiichi nuclear power plant simulated numerically by a regional ocean model. *J. Environ. Radioact.* **2012**, *111*, 100–108. [CrossRef] [PubMed]
8. Dvorzhak, A.; Puras, C.; Montero, M.; Mora, J.C. Spanish experience on modeling of environmental radioactive contamination due to Fukushima Daiichi NPP accident using JRODOS. *Environ. Sci. Technol.* **2012**, *46*, 11887–11895. [CrossRef]
9. Masumoto, Y.; Miyazawa, Y.; Tsumune, D.; Kobayashi, T.; Estournel, C.; Marsaleix, P.; Lanerolle, L.; Mehra, A.; Garraffo, Z.D. Oceanic dispersion simulation of Cesium-137 from Fukushima Dai-ichi nuclear power plant. *Elements* **2012**, *8*, 207–212. [CrossRef]
10. Periáñez, R. Models for predicting the transport of radionuclides in the Red Sea. *J. Environ. Radioact.* **2020**, *223–224*, 106396. [CrossRef]

11. Periáñez, R. APERTRACK: A particle-tracking model to simulate radionuclide transport in the Arabian/Persian Gulf. *Progr. Nucl. Energ.* **2021**, *142*, 103998. [CrossRef]
12. Periáñez, R. A Lagrangian tool for simulating the transport of chemical pollutants in the Arabian/Persian Gulf. *Modelling* **2021**, *2*, 675–685. [CrossRef]
13. Maderich, V.; Bezhenar, R.; Kovalets, I.; Khalchenkov, O.; Brovchenko, I. Long–Term Contamination of the Arabian Gulf as a Result of Hypothetical Nuclear Power Plant Accidents. *J. Mar. Sci. Eng.* **2023**, *11*, 331. [CrossRef]
14. Periáñez, R.; Min, B.-I.; Suh, K.-S. The transport, effective half-lives and age distributions of radioactive releases in the northern Indian Ocean. *Mar. Pollut. Bull.* **2021**, *169*, 112587. [CrossRef] [PubMed]
15. Tsabaris, C.; Tsiaras, K.; Eleftheriou, G.; Triantafyllou, G. ^{137}Cs ocean distribution and fate at East Mediterranean Sea in case of a nuclear accident in Akkuyu Nuclear Power Plant. *Progr. Nucl. Energ.* **2021**, *139*, 103879. [CrossRef]
16. Tsabaris, C.; Eleftheriou, G.; Tsiaras, K.; Triantafyllou, G. Distribution of dissolved ^{137}Cs, ^{131}I and ^{238}Pu at eastern Mediterranean Sea in case of hypothetical accident at the Akkuyu nuclear power plant. *J. Environ. Radioact.* **2022**, *251–252*, 106964. [CrossRef] [PubMed]
17. Periáñez, R.; Cortés, C. A Numerical model to simulate the transport of radionuclides in the Western Mediterranean after a nuclear accident. *J. Mar. Sci. Eng.* **2023**, *11*, 169. [CrossRef]
18. Periáñez, R.; Bezhenar, I.; Brovchenko, C.; Duffa, M.; Iosjpe, K.T.; Jung, T.; Kobayashi, F.; Lamego, V.; Maderich, B.I.; Min, H.; et al. Modelling of marine radionuclide dispersion in IAEA MODARIA program: Lessons learnt from the Baltic Sea and Fukushima scenarios. *Sci. Total Environ.* **2016**, *569–570*, 594–602. [CrossRef]
19. IAEA. *Modelling of Marine Dispersion and Transfer of Radionuclides Accidentally Released from Land Based Facilities*; IAEA–TECDOC–1876; IAEA: Vienna, Austria, 2019.
20. Periáñez, R.; Bezhenar, R.; Brovchenko, I.; Duffa, C.; Iosjpe, M.; Jung, K.T.; Kobayashi, T.; Liptak, L.; Little, A.; Maderich, V.; et al. Marine radionuclide transport modelling: Recent developments, problems and challenges. *Environ. Modell. Softw.* **2019**, *122*, 104523. [CrossRef]
21. Schonfeld, W. Numerical simulation of the dispersion of artificial radionuclides in the English Channel and the North Sea. *J. Mar. Syst.* **1995**, *6*, 529–544. [CrossRef]
22. Nakano, H.; Motoi, T.; Hirose, K.; Aoyama, M. Analysis of ^{137}Cs concentration in the Pacific using a Lagrangian approach. *J. Geophys. Res.* **2010**, *115*, C06015.
23. Periáñez, R.; Bezhenar, R.; Brovchenko, I.; Jung, K.T.; Kamidara, Y.; Kim, K.O.; Kobayashi, T.; Liptak, L.; Maderich, V.; Min, B.I.; et al. Fukushima ^{137}Cs releases dispersion modelling over the Pacific Ocean. Comparisons of models with water, sediment and biota data. *J. Environ. Radioact.* **2019**, *198*, 50–63. [CrossRef] [PubMed]
24. Bezhenar, R.; Heling, R.; Ievdin, I.; Iosjpe, M.; Maderich, V.; Willemsen, S.; de With, G.; Dvorzhak, A. Integration of marine food chain model POSEIDON in JRODOS and testing versus Fukushima data. *Radioprotection* **2016**, *51*, S137–S139. [CrossRef]
25. Periáñez, R.; Qiao, F.; Zhao, C.; de With, G.; Jung, K.-T.; Sangmanee, C.; Wang, G.; Xia, C.; Zhang, M. Opening Fukushima floodgates: Modelling ^{137}Cs impact in marine biota. *Mar. Pollut. Bull.* **2021**, *170*, 112645. [CrossRef] [PubMed]
26. Bezhenar, R.; Jung, K.T.; Maderich, V.; Willemsen, S.; de With, G.; Qiao, F. Transfer of radiocaesium from contaminated bottom sediments to marine organisms through benthic food chains in post–Fukushima and post–Chernobyl periods. *Biogeosciences* **2016**, *13*, 3021–3034. [CrossRef]
27. Bezhenar, R.; Kim, K.O.; Maderich, V.; de With, G.; Jung, K.T. Multi–compartment kinetic–allometric (MCKA) model of radionuclide bioaccumulation in marine fish. *Biogeosciences* **2021**, *18*, 2591–2607. [CrossRef]
28. Maderich, V.; Bezhenar, R. Heling, R.; de With, G.; Jung K.T.; Myoung, J.G.; Cho, Y.K.; Qiao, F.; Robertson, L. Regional long–term model of radioactivity dispersion and fate in the Northwestern Pacific and adjacent seas: Application to the Fukushima Dai–ichi accident. *J. Environ. Radioact.* **2014**, *131*, 4–18. [CrossRef]
29. Maderich, V.; Jung, K.T.; Bezhenar, R.; de With, G.; Qiao, F.; Casacuberta, N.; Masque, P.; Kim, Y.H. Dispersion and fate of ^{90}Sr in the Northwestern Pacific and adjacent seas: Global fallout and the Fukushima Dai–ichi accident. *Sci. Total Environ.* **2014**, *494–495*, 261–271. [CrossRef]
30. Maderich, V.; Bezhenar, R.; Tateda, Y.; Aoyama, M.; Tsumune, D.; Jung, K.T.; de With, G. The POSEIDON–R compartment model for the prediction of transport and fate of radionuclides in the marine environment. *MethodsX* **2018**, *5*, 1251–1266. [CrossRef]
31. De With, G.; Bezhenar, R.; Maderich, V.; Yevdin, Y.; Iosjpe, M.; Jung, K.T.; Qiao, F.; Periáñez, R. Development of a dynamic food chain model for assessment of the radiological impact from radioactive releases to the aquatic environment. *J. Environ. Radioact.* **2021**, *233*, 106615. [CrossRef]
32. Bleck, R. An oceanic general circulation model framed in hybrid isopycnic–Cartesian coordinates. *Ocean Model.* **2001**, *4*, 55–88. [CrossRef]
33. Xu, X.; Chassignet, E.P.; Price, J.F.; Özgökmen, T.M.; Peters, H. A regional modeling study of the entraining Mediterranean outflow. *J. Geophys. Res.* **2007**, *112*, C12005. [CrossRef]
34. Kara, A.B.;Wallcraft, A.J.; Martin, P.J.; Pauley, R.L. Optimizing surface winds using QuikSCAT measurements in the Mediterranean Sea during 2000–2006. *J. Mar. Syst.* **2009**, *78*, S119–S131. [CrossRef]
35. IAEA. *Sediment Distribution Coefficients and Concentration Factors for Biota in the Marine Environment*; Technical Reports Series 422; IAEA: Vienna, Austria, 2004.

36. Nyffeler, U.P.; Li, Y.H.; Santschi, P.H. A kinetic approach to describe trace element distribution between particles and solution in natural aquatic systems. *Geochim. Cosmochim. Acta* **1984**, *48*, 1513–1522. [CrossRef]
37. Periáñez, R.; Brovchenko, I.; Duffa, C.; Jung, K.T.; Kobayashi, T.; Lamego, F.; Maderich, V.; Min, B.I.; Nies, H.; Osvath, I.; et al. A new comparison of marine dispersion model performances for Fukushima Dai–ichi releases in the frame of IAEA MODARIA program. *J. Environ. Radioact.* **2015**, *150*, 247–269. [CrossRef]
38. Periáñez, R.; Suh, K.S.; Min, B.I.; Villa, M. The behaviour of ^{236}U in the North Atlantic Ocean assessed from numerical modelling: A new evaluation of the input function into the Arctic. *Sci. Total Environ.* **2018**, *626*, 255–263. [CrossRef]
39. Periáñez, R.; Suh, K.S.; Min, B.I. The behaviour of ^{137}Cs in the North Atlantic Ocean assessed from numerical modelling: Releases from nuclear fuel reprocessing factories, redissolution from contaminated sediments and leakage from dumped nuclear wastes. *Mar. Pollut. Bull.* **2016**, *113*, 343–361. [CrossRef]
40. Periáñez, R.; Bezhenar, R.; Iosjpe, M.; Maderich, V.; Nies, H.; Osvath, I. Outola, I.; de With G. A comparison of marine radionuclide dispersion models for the Baltic Sea in the frame of IAEA MODARIA program. *J. Environ. Radioact.* **2015**, *139*, 66–77. [CrossRef]
41. Kobayashi, T.; Nagai, H.; Chino, M.; Kawamura, H. Source term estimation of atmospheric release due to the Fukushima Dai–ichi Nuclear Power Plant accident by atmospheric and oceanic dispersion simulations. *J. Nucl. Sci. Technol.* **2013**, *50*, 255–264. [CrossRef]
42. Christoudias, T.; Lelieveld, J. Modelling the global atmospheric transport and deposition of radionuclides from the Fukushima Dai–ichi nuclear accident. *Atmos. Chem. Phys.* **2013**, *13*, 1425–1438. [CrossRef]
43. IAEA MARIS. *Marine Radioactivity Information System*; Division of IAEA Environment Laboratories: Monaco, 2023. Available online: https://maris.iaea.org (accessed on 30 April 2023).
44. Uddin, S.; Fowler, S.W.; Behbehani, M.; Al–Ghadban, A.N.; Swarzenski, P.W.; Al–Awadhi, N. A review of radioactivity in the Gulf region. *Mar. Pollut. Bull.* **2020**, *159*, 111481. [CrossRef] [PubMed]
45. Vives i Batlle, J.; Beresford, N.; Beaugelin–Seiller, K.; Bezhenar, R.; Brown, J.; Cheng, J.-J.; Cujic, M.; Dragovic, S.; Duffa, C.; Fievet, B.; et al. Inter-comparison of dynamic models for radionuclide transfer to marine biota in a Fukushima accident scenario. *J. Environ. Radioact.* **2016**, *153*, 31–50. [CrossRef] [PubMed]
46. Periáñez, R. Viewpoint on the Integration of Geochemical Processes into Tracer Transport Models for the Marine Environment. *Geosciences* **2022**, *12*, 152. [CrossRef]
47. Periáñez, R.; Suh, K.S.; Min, B.I.; Casacuberta, N.; Masqué, P. Numerical modelling of the releases of ^{90}Sr from Fukushima to the ocean: An evaluation of the source term. *Environ. Sci. Technol.* **2013**, *47*, 12305–12313. [CrossRef]
48. Sartandel, S.J.; Jha, S.K.; Tripathi, R.M. Latitudinal variation and residence time of ^{137}Cs in Indian coastal environment. *Mar. Pollut. Bull.* **2015**, *100*, 489–494. [CrossRef] [PubMed]
49. Zinger, I.; Oughton, D.H.; Jones, S.R. Stakeholder interaction within the ERICA Integrated Approach. *J. Environ. Radioact.* **2008**, *99*, 1503–1509. [CrossRef]